

NeuroLens: Augmented Reality-based Contextual Guidance through Surgical Tool Tracking in Neurosurgery

Sangjun Eom*
Department of Electrical and
Computer Engineering
Duke University

David Sykes†
School of Medicine
Duke University

Shervin Rahimpour‡
Department of Neurosurgery
University of Utah

Maria Gorlatova§
Department of Electrical and
Computer Engineering
Duke University

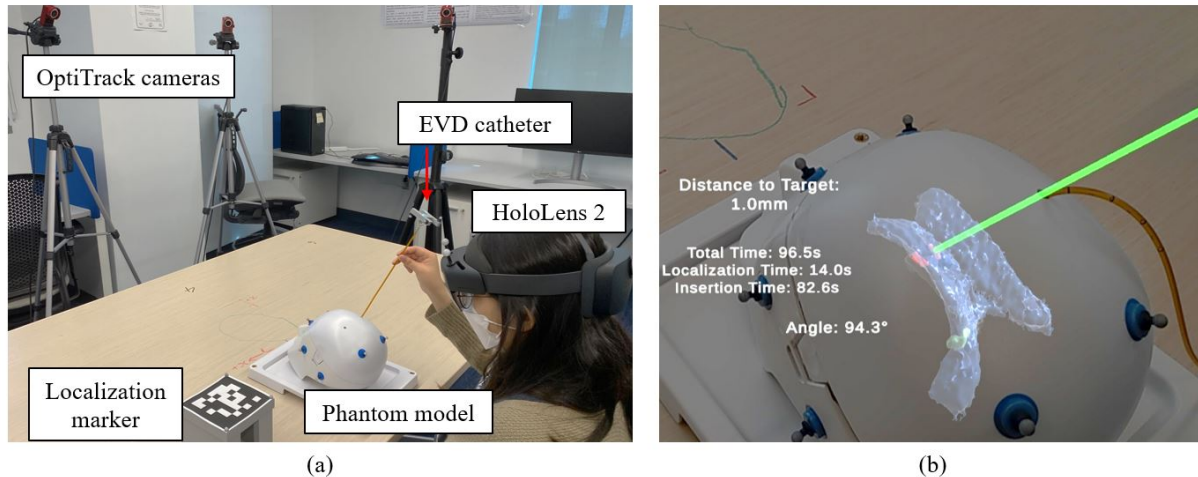


Figure 1: The overall setup of NeuroLens (a) and AR-based contextual guidance during the EVD procedure (b).

ABSTRACT

External ventricular drain (EVD) is a common, yet challenging neurosurgical procedure of placing a catheter into the brain ventricular system that requires prolonged training for surgeons to improve the catheter placement accuracy. In this paper, we introduce NeuroLens, an Augmented Reality (AR) system that provides neurosurgeons with guidance that aids them in completing an EVD catheter placement. NeuroLens builds on prior work in AR-assisted EVD to present a registered hologram of a patient’s ventricles to the surgeons, and uniquely incorporates guidance on the EVD catheter’s trajectory, angle of insertion, and distance to the target. The guidance is enabled by tracking the EVD catheter. We evaluate NeuroLens via a study with 33 medical students, in which we analyzed students’ EVD catheter insertion accuracy and completion time, eye gaze patterns, and qualitative responses. Our study, in which NeuroLens was used to aid students in inserting an EVD catheter into a realistic phantom model of a human head, demonstrated the potential of NeuroLens as a tool that will aid and educate novice neurosurgeons. On average, the use of NeuroLens improved the EVD placement accuracy of year 1 students by 39.4% and of the year 2–4 students by 45.7%. Furthermore, students who focused more on NeuroLens-provided contextual guidance achieved better results.

Index Terms: Human-centered computing—Human computer interaction (HCI)—Interaction paradigms—Mixed / augmented reality; Human-centered computing—Human computer interaction (HCI)—Interaction devices—Displays and imagers;

*e-mail: sangjun.eom@duke.edu

†e-mail: david.sykes@duke.edu

‡e-mail: shervin.rahimpour@hsc.utah.edu

§e-mail: maria.gorlatova@duke.edu

1 INTRODUCTION

The external ventricular drain (EVD) is a common neurosurgical procedure for patients with hydrocephalus, meningitis, and traumatic injury [23]. In EVD, the cerebrospinal fluid is drained to relieve pressure buildup within the skull by placing a catheter into the brain ventricular system, via a small opening in the skull. Despite being practiced more than 20,000 times annually in the U.S. [26], the challenges of the EVD procedure come from relying on the surgeon’s expertise and the external anatomical landmarks of the patients to estimate the target. The EVD catheter placement is often performed at the bedside without any aides (‘freehand’). This procedure’s success rate is around 73% [36]; the success rate is lower for less experienced surgeons [27]. A misplacement of the EVD can lead to serious complications such as ventriculitis, brain abscesses, or subdural empyema [11]. Thus, prolonged training [25] or guidance of computed tomography (CT) scan [2] is required to improve the catheter placement accuracy of this ‘freehand’ approach.

Due to these challenges, EVD is a prime example of a neurosurgical procedure that can benefit from the integration of Augmented Reality (AR), guiding surgeons in a more convenient and intuitive manner [5]. The anatomical visualization in AR substantially enhances the surgeon’s perception of the surgical environment [22] and increases confidence regarding precision [15] during the procedure where the surgeon’s field of view is often limited. To provide guidance to surgeons via anatomical visualization, marker-based image registration has been adopted in several lines of work that integrated AR and EVD [19, 31, 39]. In these systems, a 3D hologram of the patient’s ventricles is rendered in the corresponding location within the skull, allowing surgeons to see the area they are targeting. Though anatomical visualization enhances the surgeon’s field of view, it provides no guidance on how to best aim the catheter.

To address this, we designed NeuroLens, *the first AR system that provided both the anatomical visualization of the patient’s ventricular hologram and contextual guidance on catheter placement* to aid novice surgeons in completing the EVD in both training and clinical settings. The AR guidance is enabled by the optical tracking of an

external 6-camera OptiTrack system and visualized in AR by the Microsoft HoloLens 2, shown in Fig. 1a. We compute the transformation of world coordinates between OptiTrack and HoloLens 2, achieving high accuracy and low latency real-time tracking of optical markers in visualizing a patient-specific 3D model.

NeuroLens integrates the contextual guidance, shown in Fig. 1b, that is enabled by tracking the EVD catheter. The guidance consists of displaying the catheter’s trajectory, angle of insertion, and distance to the target. In addition, we employ voice commands for surgeons to intraoperatively initiate and complete the procedure with ease, and personalize the anatomical visualization based on their needs. We evaluate NeuroLens via an Institutional Review Board (IRB)-approved study with 33 medical students, in which we analyze students’ EVD catheter insertion accuracy and completion time, eye gaze patterns, and qualitative responses (Section 4). Our contributions are as follows:

- We design an optical marker-based AR system using 6 OptiTrack cameras and Microsoft HoloLens 2 for intraoperative use in neurosurgery. Our approach reduces image registration error to 1.17mm, outperforming state-of-the-art fiducial marker-based methods (Section 3).
- We integrate AR-based contextual guidance to aid surgeons in catheter targeting by displaying, in real-time, the distance to the target, the angle of insertion, and the catheter projection. We also develop a phantom model that reflects human anatomy and emulates brain texture to evaluate NeuroLens in more realistic settings (Section 3). Our user study shows that the participants agreed or strongly agreed with the usefulness of contextual guidance (97%) and the phantom model for learning (93.9%) (Section 5).
- Our study demonstrated that NeuroLens improves students’ accuracy compared to an unassisted (‘freehand’) EVD procedure. The study also revealed important differences in the behavior of groups of students that achieved the best and the worst accuracy in NeuroLens-assisted EVD trials: specifically, we observed that the best-performing group took longer to complete the procedure, and focused on the contextual guidance substantially more than the worst-performing group (Section 5).

We first describe related work on image registration, tool tracking, and contextual guidance with AR in medical domains in Section 2. Then, we lay out the overall architecture in Section 3 and user study design in Section 4. We analyze the user study results in Section 5. Discussion and future work, then conclusions are followed in Sections 6 and 7, accordingly.

2 RELATED WORK

Marker-based image registration and tool tracking. Fiducial and optical marker-based tracking is a common approach to detect the position and orientation of an object in a surgical application. In AR-assisted surgery, marker-based tracking has been employed in the tracking of a surgical robot arm [29] and image registration of anatomical visualization in various types of surgery (e.g., open surgery [1], neurosurgery [9, 14, 32]). Prior work that used fiducial markers reported image registration error ranging from 2.5mm to 8.5mm [8, 31] with drifts over time [9, 31]; with optical markers, smaller registration error of 1mm to 2mm was reported [7]. It is challenging to use fiducial markers for tracking a surgical tool, in particular, due to the heightened sensitivity of fiducial marker detection algorithms to the angle and the distance between the AR device and the marker [4]. Hence, we design NeuroLens to rely on optical markers, with 360 degrees of field of view from 6 OptiTrack cameras surrounding the surgical area.

AR-assisted EVD. To improve the freehand EVD catheter placement accuracy, several researchers have developed systems that use

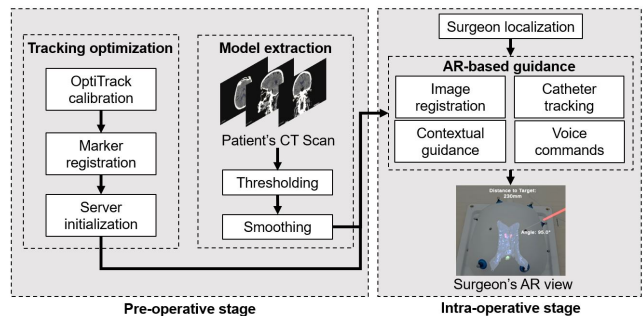


Figure 2: Overall architecture of NeuroLens.

AR to render a registered hologram of patient’s ventricles, enabling the surgeon to see the location they are targeting [7, 19, 31, 39]. A system for both cranial biopsy and EVD, reporting a sub-millimeter accuracy level, was proposed by [33], however the system did not use a head-mounted AR device, and the needle was used instead of the catheter for placement. This work has shown promising results – e.g., [39] demonstrated, in a study with 8 medical students, the average accuracy of 19.9mm for a freehand procedure and 11.9mm for an AR-assisted one – but much room for improvement remains, particularly for assisting surgeons with less experience in the procedure. NeuroLens improves upon the registration accuracy results reported in prior work, and integrates additional guidance to aid surgeons who are learning the procedure. Additionally, our evaluation of NeuroLens’s AR assistance for EVD more than doubles the number of participants compared to prior work (33 in our study vs. 8–15 in [19, 31, 39]), allowing us to draw unique insights about the differences in performance of different user groups.

AR-based contextual guidance. Coupling AR-based visualizations of a patient’s anatomy with additional contextual information about the surgical task has the potential to reduce the surgeon’s cognitive workload and improve the outcomes of AR-supported surgeries [41]. Different types of domain-specific contextual guidance have been demonstrated for AR-supported endodontic [35], dental implant [17], and orthopedic [38] surgeries. NeuroLens uniquely provides AR-based contextual guidance for EVD; we assess the impact of this guidance via quantitative and qualitative measures of surgeons’ performance, experience, and engagement with different elements of the guidance.

3 OVERALL ARCHITECTURE

Fig. 2 shows our overall architecture in two stages. In the pre-operative stage, optimization of OptiTrack tracking and extraction of a patient-specific ventricular hologram are completed. In the intra-operative stage, the surgeon localizes for computing the transformation of world coordinates, then initiates the AR-based guidance.

3.1 System Setup

NeuroLens uses the HoloLens 2 as the AR headset, and six Flex 3 OptiTrack cameras with lens specs of 57.5 degrees in the field of view and 800nm of a long-pass infrared range for real-time tracking. The OptiTrack cameras are evenly distributed around the table to capture full 360 degrees of an angular view for stable and accurate tracking of the optical markers. We use the OptiTrack cameras to track four objects including the HoloLens 2, the phantom model, the localization marker, and the EVD catheter, as shown in Fig. 3.

Transformation of world coordinates. HoloLens 2 and OptiTrack operate in different world coordinates, thus a transformation between those two coordinate systems is required. To compute the transformation of the world coordinates, both HoloLens 2 and OptiTrack locate the same target that serves as a reference point, a common approach to calculating the differences in coordinate systems when relying on an external optical tracking system [12, 30, 40].

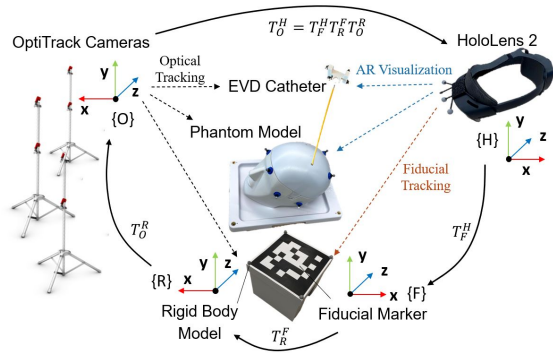


Figure 3: System setup and transformation of world coordinate systems between OptiTrack and HoloLens 2.

We created a 12cm by 12cm square 2D fiducial marker as a localization target. This localization marker is detected by the HoloLens 2 Vuforia marker detection, which reported higher accuracy in registration error when compared to other detection methods (e.g., ARToolKit) [7], to obtain both the position and the orientation of the marker. Four optical markers were attached to the corners of the localization marker to be tracked by the OptiTrack system. The transformation of the world coordinates is shown in Eq. 1, where T_F^H is obtained by Vuforia marker detection on HoloLens 2, T_R^F is the transformation between the fiducial marker and a rigid-body of the optical marker, and T_O^R is obtained by OptiTrack’s tracking of the localization marker:

$$T_O^H = T_F^H T_R^F T_O^R. \quad (1)$$

By computing the transformation of the world coordinates, NeuroLens ensures the robustness of the system through high accuracy of image registration and low latency of data communication between OptiTrack and HoloLens 2. The image registration error was calculated by running 15 trials of measuring differences in the displacement between the phantom model and the hologram in each axis with a digital caliper. The average image registration error of the three axes was 1.17mm. The average latency of data communication between OptiTrack and HoloLens 2 was 12.32ms. This improves upon prior work on image registration using a fiducial marker tracking [8, 31] that reports over 2mm of registration error.

Patient-specific ventricular hologram. To achieve a more realistic target of ventricular hologram in AR, we extracted a sample model of brain ventricles from an anonymous patient’s computer tomography (CT) scan. Using 3D Slicer software, we applied a threshold to extract the ventricles, a smoothing filter to render the 3D ventricular model, and labeling of each ventricular part on the model. Our ventricular model, shown in Fig. 4a, includes a lateral ventricle, two foramen of Monro, a third ventricle, and a cerebral aqueduct. The right foramen of Monro was used as a target point of the catheter placement during the user study.

3.2 Phantom Model

We created the phantom model, shown in Fig. 3, to be anatomically similar to a patient’s head for testing, analysis, and evaluation of our system. We attached eight optical markers to the phantom model to facilitate real-time tracking by the OptiTrack system. We pre-drilled holes on the skull corresponding to Kocher’s points which are the external landmarks that serve as entry points for the EVD catheter placement. A 3D printable brain mold was designed to be placed within the phantom model where a metal bead was located at a target of the foramen of Monro. This allowed the accuracy of catheter placement to be analyzed by measuring the distance between the tip of the catheter and the foramen of Monro on a post-experiment

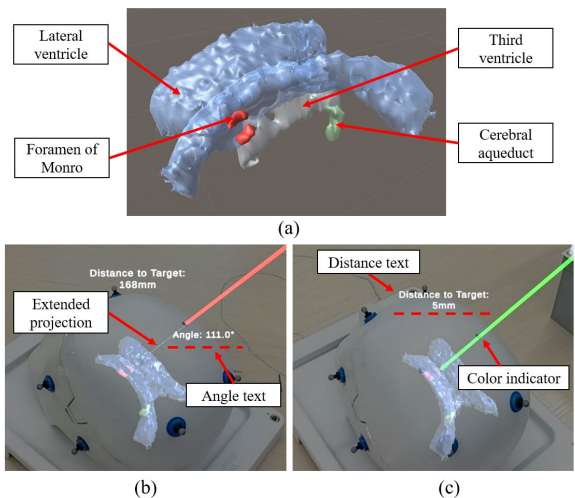


Figure 4: Patient-specific ventricular hologram consisting of four different parts (a); AR-based contextual guidance estimating catheter trajectory (b) and targeting foramen of Monro (c).

micro CT scan. The CT scans can be used to visualize both the catheter tip and radiopaque foramen of Monro (additional details are provided in Section 5).

To simulate a realistic, brain-like texture within the mold, the mold was filled with an agarose gel, commonly used for electrophoresis in biochemistry, made from a solution of molecular biology grade agarose powder and water at a ratio that was optimized for creating a firm texture. This solution was firm enough to hold the catheter, yet still penetrable, hence it provided texture feedback during the catheter insertion. The solution for a single mold was made by combining 2.70g of agarose powder with 360ml of water. The solution was stirred, and then heated to boil, allowing the agarose to dissolve. This solution was cooled for approximately 30 minutes before being poured into the mold, where it was left to solidify for 120 minutes. The entire process took about 160 minutes per mold.

3.3 Voice Recognition and Personalization

We use the built-in voice recognition on HoloLens 2 to allow surgeons to initialize, complete the EVD procedure, and personalize the anatomical visualization of a ventricular hologram. The surgeons use the voice command, “start,” to compute the transformation of world coordinates when a fiducial marker was detected. The user initiative was necessary due to the possibility of incorrect detection of a fiducial marker which can cause an incorrect transformation of the world coordinates. Therefore, we allowed the surgeon to determine a correct position and orientation of a white cube overlaid on the marker, then proceeded to compute the transformation. When the catheter placement was completed, the surgeons use the voice command, “complete,” to record the resulting catheter placement before removing the inner stylet.

We also provide a list of voice commands to allow surgeons to personalize the anatomical visualization of a ventricular hologram based on their needs. Often, when complicated medical information is visualized in AR, the surgeon’s view could be obstructed, hence the obstruction of view could make it harder to visualize the target. This could potentially increase discomfort such as fatigue from the visualization. By default, all four parts of the hologram, shown in Fig. 4a, are visualized; however, we allow surgeons to hide its parts by using the voice command, “hide,” followed by the name of the parts such as the “third ventricle” or the “lateral ventricle”.

3.4 Tool Tracking and Contextual Guidance

We integrated AR-based contextual guidance by tracking the EVD catheter to aid the catheter projection and the targeting of the for-

men of Monro.

Catheter tracking. The EVD catheter is a thin flexible tube about 36cm in length and 3mm in diameter. An inner stylet is inserted inside the catheter to provide stiffness to the catheter placement task. Attaching optical markers to a catheter itself is impractical because of its dimensions and elasticity. Thus, we designed an H-shape 3D-printed mount with the dimensions of 50mm by 50mm by 10mm to be latched at the top of the inner stylet, shown in Fig. 2. We attached four optical markers to each corner of the H-shape to provide enough distance between markers to avoid occlusions or false positive tracking of the markers.

Aiding catheter projection. During the insertion of the catheter through a skull, the direction of the catheter is critical to determining whether the catheter will hit the foramen of Monro. However, due to the limited field of view inside the skull, the surgeons face difficulties in estimating a catheter trajectory that lines up with the target. We create an AR visualization of an extended line of a catheter projection as a white dotted line in a 3D hologram to aid the surgeons. This helps surgeons in estimating the catheter projection inside the skull and aligning the catheter to be in line with the target, as shown in Fig. 4b.

Another contextual element is a textual indicator of the angle, θ , between the catheter hologram and the surface of the skull. This angle of catheter insertion determines whether the trajectory of the catheter is in line with the foramen of Monro. The approximate angle of catheter trajectory for a freehand EVD is about 90 degrees to the surface of the skull [11]. We use Eq. 2 to calculate this insertion angle relative to the skull by using vectors of catheter hologram, v_c , and the surface of the skull, v_s .

$$\theta = \cos^{-1} \left(\frac{v_c \cdot v_s}{|v_c| \times |v_s|} \right). \quad (2)$$

We visualize the angle as a textual indicator in AR below Kocher's point, as shown in Fig. 4b.

Targeting the foramen of Monro. While visualizing the catheter projection guides the surgeons in determining the right insertion angle of the catheter, we also display the depth of catheter insertion by calculating the Euclidean distance $d(C, T)$ between the tip of the catheter, (x_c, y_c, z_c) , and the foramen of Monro, (x_t, y_t, z_t) , using Eq. 3, and displaying this distance as a textual indicator above the ventricular hologram, as shown in Fig. 4c.

$$d(C, T) = \sqrt{(x_c - x_t)^2 + (y_c - y_t)^2 + (z_c - z_t)^2}. \quad (3)$$

With this textual indicator, surgeons no longer need to read the depth label physically marked on the catheter, and can instead maintain their focus on the surgical area.

Another contextual element comes from a color indicator of the catheter hologram that shows whether the foramen of Monro is in line with the catheter projection. To calculate the distance from the foramen of Monro to the catheter projection, $d(C_t, C_b, T)$, a point to line Eq. 4 is used, where C_t is the 3D coordinate of the top of the catheter, C_b is the 3D coordinate of the tip of the catheter, and T is the 3D coordinate of the foramen of Monro.

$$d(C_t, C_b, T) = \frac{|(C_t - T) \times (C_t - C_b)|}{|C_b - T|}. \quad (4)$$

The threshold of the distance is set to 2mm. This means when $d(C_t, C_b, T) < 2\text{mm}$, the catheter hologram changes the color to green to indicate that the catheter is projected to end up in close proximity to the foramen of Monro. When $d(C_t, C_b, T) > 2\text{mm}$, the color of the catheter hologram stays red.

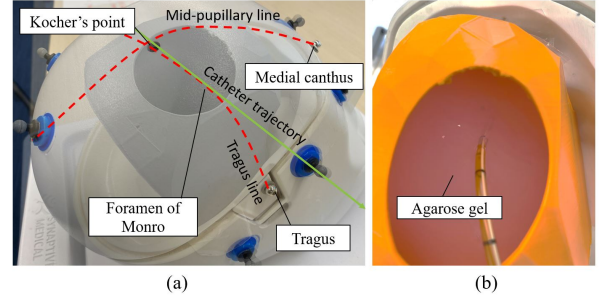


Figure 5: Anatomical landmarks on the phantom model (a) and agarose gel poured inside the mold for texture feedback (b).

4 USER STUDY DESIGN

Our study, approved by the Duke University IRB, is centered on medical students performing one freehand EVD trial, followed by one AR-assisted EVD trial. Prior to each trial, each participant is provided with an instructional video. The goal of the user study is to evaluate the impact of AR assistance in EVD in training medical students without prior knowledge of the EVD. We recruited medical students by emailing the medical schools in Duke University and the University of North Carolina at Chapel Hill.

4.1 EVD Trials

Freehand EVD. The steps for freehand placement of an EVD are as follows. Kocher's point is approximated by locating two key anatomical landmarks: the tragus and the medial canthus as shown in Fig. 5. The point on the skull in which a sagittal plane through the medial canthus intersects a coronal plane through the tragus defines Kocher's point. Next, the target point of the foramen of Monro is approximated by angling the catheter tip from Kocher's point towards the contralateral medial canthus. The catheter is inserted approximately 7cm towards the target, and finally, the inner stylet is removed. These steps are described to participants in an instructional video¹ recorded by a neurosurgeon with 8 years of clinical experience. The instructional video is 90 seconds long.

AR-assisted EVD. The steps of an AR-assisted EVD are as follows. First, eye calibration on HoloLens 2 is performed for rendering holograms at accurate locations and collecting accurate eye gaze data. Upon the initialization of the AR app on HoloLens 2, the localization marker is detected for computing the transformation of world coordinates. The AR visualization and guidance are initiated through a voice command issued by the user. Next, the catheter is inserted into a target point, and finally, the inner stylet is removed. These steps are described to participants in an instructional video² created by a team with a combination of AR and neurosurgical expertise. The instructional video is 180 seconds long.

4.2 Survey Questions

The pre-experiment and post-experiment surveys are given to each participant to fill out before and after the user study. In the pre-experiment survey, we ask demographic questions about prior experience in AR and EVD. We assemble a set of questions in different categories for the post-experiment survey, shown in Table 1.

Five categories in the post-experiment survey are: AR visualization, contextual guidance, AR experience, surgical experience, and physical discomfort. For the category of AR visualization (Q1–Q4), we ask the participants if each hologram was realistic and overall visualization was useful for learning. For the category of contextual

¹The instructional video of a freehand EVD is provided at <https://sites.duke.edu/sangjuneom/freehandevd/>

²The instructional video of an AR-assisted EVD is provided at <https://sites.duke.edu/sangjuneom/arassistedevd/>

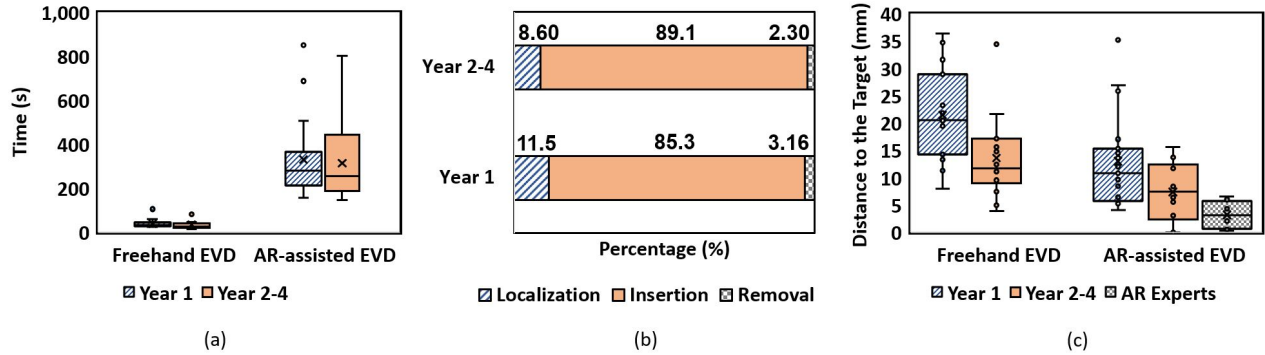


Figure 6: Average total EVD completion time (a), average percentage of total time spent on each task (b), and average accuracy in catheter distance to the target (c).

Table 1: Post-experiment survey questions.

	Questions
Q1	The ventricular hologram in AR environment was realistic.
Q2	The catheter hologram in AR environment was realistic.
Q3	The positioning of the foramen of Monro in AR environment was realistic.
Q4	The overall AR-based visualization was useful for learning about the neurosurgical procedure.
Q5	The extended projection of catheter (a white dotted line) in AR environment was useful.
Q6	The color indicator of catheter projection (red/green catheter holograms) in AR environment was useful.
Q7	The text showing distance from the tip of catheter to foramen of Monro in AR environment was useful.
Q8	The text showing the angle between the catheter projection and surface of the phantom model in AR environment was useful.
Q9	The voice commands in AR environment were useful.
Q10	The personalization of hologram (e.g. hiding and showing parts of ventricular hologram via voice commands based on personal needs) was useful.
Q11	The overall AR-based contextual guidance was useful for learning about the neurosurgical procedure.
Q12	The hologram visualization was robust without significant lagging.
Q13	The hologram visualization was robust without significant drift or jump.
Q14	The hologram visualization didn't obstruct my view.
Q15	The phantom model was realistic.
Q16	The texture feedback (during catheter insertion procedure) inside the phantom model was realistic.
Q17	The use of phantom models was useful for learning about the neurosurgical procedure.
Q18	AR guidance will be helpful in clinical settings intraoperatively.
Q19	I didn't feel tired or fatigued at some point during the experiment.
Q20	I didn't feel dizziness at some point during the experiment.
Q21	I didn't feel discomfort with AR headset at some point during the experiment.
Q22	What was the most challenging task of the external ventricular drain procedure?
Q23	If you have any other comments or feedback about your experience, please write below.

guidance (Q5–Q11), we ask the participants if each type of contextual guidance was useful and overall contextual guidance was useful for learning. For the categories of AR (Q12–Q14) and surgical experiences (Q15–Q18), we ask the participants if the system was robust without lagging, drift, and obstruction of view, and the phantom model was useful for learning. For the category of physical discomfort (Q19–Q21), we ask the participants if they experienced fatigue, dizziness, and discomfort. All questions in these five cate-

gories are answered on a five-point Likert scale. At the end of the survey, we ask the participants to identify the most challenging task of the EVD and to leave any open-ended feedback about the overall experience (Q22 and Q23).

4.3 Data Collection

During both freehand and AR-assisted EVD trials, we collect data on the total completion time of the procedure and the accuracy of the catheter distance to the target. Additionally, during the AR-assisted trials, we capture the participants' eye gaze distribution.

Total completion time. We measure the total completion time of the freehand EVD trial by a stopwatch from the moment that the participant starts identifying the anatomical landmarks to the removal of the inner stylet. The total completion time of the AR-assisted EVD trial is measured by the system from the moment that the AR app is initialized to the removal of the inner stylet.

Distance to the target. To obtain an accurate result of catheter placement from the target inside the mold, we use a Nikon XTH 225 ST, a high-resolution micro X-ray CT scanner [34], to capture the full volume of the mold. After we obtain a sequence of more than one thousand slices of CT images, we visualize them in the 3D graphical software, Avizo, to render the 3D volume. The accuracy is calculated by measuring the Euclidean distance from the target point of the metal bead to the tip of the catheter.

Eye gaze distribution. We enable the built-in gaze tracking on HoloLens 2 to collect the gaze direction during each AR-assisted EVD trial. Using the gaze direction, we calculate the gaze hit point on the hologram to measure the distribution of the participant's gaze focus. We segment the holograms into four categories of the ventricle, the EVD catheter, the distance text, and the angle text, and analyze the distribution of the participant's gaze focus on each category.

4.4 Participant Selection

We recruited 33 medical students from Duke University and the University of North Carolina at Chapel Hill, each conducting one freehand trial and one AR-assisted trial. We had 19 year 1 students and 14 year 2–4 students with clinical experience. All 33 students had no knowledge of the EVD procedure. One of them uses the AR headset infrequently, less than once a week, 15 had worn an AR headset once or twice, and 17 had never worn an AR headset before. 20 of them wore glasses for nearsightedness and 13 did not; none of the participants had any other eyesight-related conditions such as strabismus or colorblindness. Additionally, to make a comparison with the data collected from the experts, we conducted 8 AR-assisted trials from two AR experts with sufficient experience in AR and EVD to collect both eye samples and accuracy data. We also conducted 4 AR-assisted trials with two surgeons with more than 8 years of clinical experience to sample their eye gaze distributions.

Table 2: Comparison of NeuroLens to other AR-assisted EVD systems.

	Gestel et al. [39]	Schneider et al. [31]	Li et al. [19]	NeuroLens (this paper)		
Image Registration	Yes	Yes	Yes	Yes		
Tool Tracking	Rigid	No	No	Non-rigid		
Contextual Guidance	No	No	No	Yes		
Hardware	HoloLens 1	HoloLens 1	HoloLens 1	HoloLens 2		
Registration Marker	Optical	Single fiducial	Manual	Optical		
Level of Expertise	Year 2–3 students	Surgeons	Surgeons	Year 1 students	Year 2–4 students	AR experts
Number of Participants	8	10	15	19	14	2
Freehand Accuracy (mm)	19.9 ± 4.2	N/A	11.26 ± 4.83	21.42 ± 8.08	13.55 ± 7.81	N/A
AR-assisted Accuracy (mm)	11.9 ± 4.7	7.1 ± 4.1	4.34 ± 1.63	12.97 ± 8.54	7.36 ± 5.55	3.12 ± 2.53
Accuracy Improvement (%)	40.2	N/A	61.5	39.4	45.7	N/A

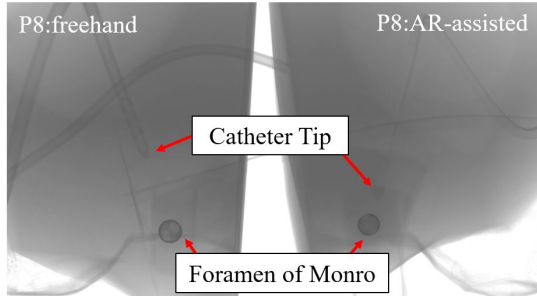


Figure 7: Sample micro CT scans from the same participant's trials: freehand (left) and AR-assisted (right).

5 RESULTS

5.1 Total Completion Time

The comparison of the total completion time for freehand and AR-assisted EVD trials is shown in Fig. 6a. Year 1 students spent more time on the freehand EVD trial (37.36s) than the year 2–4 students (34.73s). Similarly, the completion time of the AR-assisted EVD trial for year 1 students (329.56s) was longer than for year 2–4 students (313.45s). There was a larger difference in the total completion times between these two groups in the AR-assisted EVD trial than in the freehand trial. We hypothesize that, since year 2–4 students had clinical experience, they were better in ensuring the accuracy of the catheter alignment and understanding each element of contextual guidance, which resulted in shorter completion times. As the AR-assisted EVD trial consists of three tasks, localization, catheter insertion, and inner stylet removal, we analyze the time distribution on these tasks; these results are shown in Fig. 6b. Overall, both year 1 and year 2–4 students spent a similar percentage of their time on the localization, insertion, and removal.

5.2 Ground Truth Accuracy

From the analysis, we found that the average Euclidean distance to the target on freehand EVD trials was 21.42mm for year 1 students and 13.55mm for year 2–4 students, as shown in Fig. 6c. *On AR-assisted trials, this distance was reduced, on average, by 39.4% for year 1 students and by 45.7% for year 2–4 students.* A sample of raw CT scan images is shown in Fig. 7. The demonstrated accuracy improvements indicate the potential of NeuroLens to aid neurosurgeons in reaching targets within the brain.

Comparison to the state of the art. Table 2 shows the comparison of our results to the state of the art [19, 31, 39]. *The accuracy levels achieved by the NeuroLens-assisted AR experts considerably improve upon the best results presented in prior work (i.e., reduce the average distance to the target by 28.1%, from 4.34mm reported in [19] to 3.12mm).* This suggests that additional practice with NeuroLens would allow surgeons and medical students to improve upon the accuracy reported in this study; we will evaluate this in our future

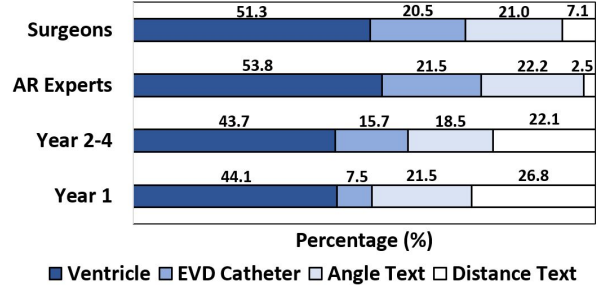


Figure 8: Eye gaze distributions across holograms.

work. Prior studies have not involved year 1 students; in our study, the extent of their accuracy improvement, between the freehand and the AR-assisted EVD trials, is at the level of the improvements observed in year 2-3 students in [39] (39.4% vs. 40.2%, correspondingly). On the absolute accuracy measurements, the year 1 students in our study performed worse than upper-year students in both prior studies and in our work. However, the year 2-4 students' accuracy in our trials (7.36mm) significantly surpasses the accuracy achieved by upper-year students (vs. 11.9mm in [39]) and is comparable to the accuracy achieved by experienced surgeons (vs. 7.1mm in [31]) in previous work. The use of newer hardware (i.e., HoloLens 2) enhanced the quality of marker-based image registration (vs. HoloLens 1 in prior work). However, we hypothesize that the integration of contextual guidance and tool tracking largely affected the improvement of the accuracy levels of the catheter placement.

5.3 Eye Gaze Distributions

From the eye gaze data collected in our user study, we calculated participants' distribution of eye gaze across the holograms; these results are shown in Fig. 8. Across all levels of expertise, the participants dedicated considerable attention to the ventricular hologram, with the average percentage of time devoted to it varying from 47.4% for year 2–4 students to 53.8% for the AR experts. *This indicates the importance of providing anatomical visualizations in AR-assisted surgery.* The extent of participants' attention dedicated to the contextual guidance presented by NeuroLens varied substantially by the participants' level of expertise: specifically, students looked at it considerably more than the experienced surgeons or the AR experts. Specifically, while the surgeons and the AR experts focused on the contextual guidance for the total of, correspondingly, 28.1% of the time (21.0% on angle text, 7.1% on distance text) and 24.7% of the time (22.2% on angle text, 2.5% on distance text), year 1 students focused on it for 48.3% of the time (21.5% on angle text, 26.8% on distance text), and year 2–4 students for 35.5% of the time (20.0% on angle text, 15.5% on distance text). This is unsurprising: it is reasonable to expect less experienced participants to rely more on the guidance provided to them. In Section 5.5, we further analyze the differences in eye gaze patterns of participants who achieve different levels of accuracy in their trials.

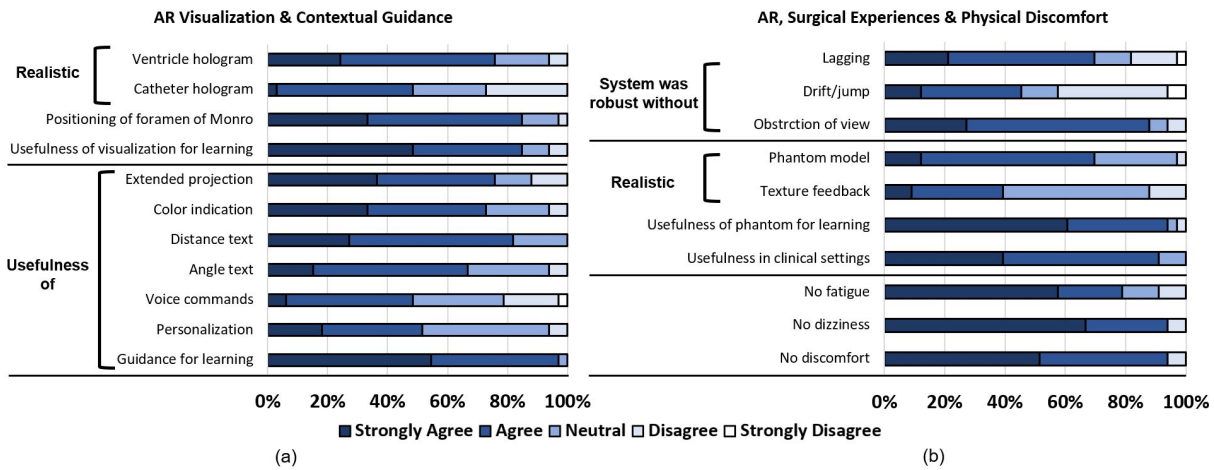


Figure 9: Survey responses on a five-point Likert scale for categories of AR visualization and contextual guidance (a), and AR experience, surgical experience, and physical discomfort (b).

5.4 Survey Responses

Our post-experiment survey responses are summarized in Fig. 9. We define *positivity rate* as the percentage of participants’ responses in the “strongly agree” and “agree” categories. The participants’ free-text responses are quoted with the participant number, *P*.

AR visualization & contextual guidance. The participants mostly agreed that the AR visualization of the ventricular hologram and positioning of the foramen of Monro was realistic (75.8% and 84.8% positivity rates, correspondingly). 84.8% of the participants agreed or strongly agreed that the overall AR visualization was useful for learning. However, only 48.5% of the participants agreed (and only 2.9% strongly agreed) that the catheter hologram was realistic. The participants also provided additional feedback that they felt aligning the catheter hologram to the real catheter (P8, P9, P10, P13, P25, P27, P28, P33) or to correct the insertion angle (P11, P21) was difficult. This was due to the non-rigid structure of the catheter, which tended to bend when the fingers holding the catheter provided too much pressure which caused misalignment of the hologram. In future work, we will explore the use of sensors (e.g., strain gauge) on the catheter to detect the non-rigidity and reflect the accurate shape of the catheter hologram.

The participants appreciated all forms of the contextual guidance we provided. The participants agreed that the contextual guidance was useful, with high positivity rates for each of the elements: distance text (81.8%), color indication (72.7%), extended projection (75.8%), and angle text (66.7%). 97% of participants agreed or strongly agreed that the provided contextual guidance was useful for learning. The participants who provided additional feedback felt that “aligning the catheter hologram with green color” (P22, P23, P24) was the most challenging contextual guidance. This was potentially due to the low threshold of color indicator or unsteady hand movement making it difficult to keep it under the threshold. In future work, we will explore altering this guidance: e.g., converting a color-based indicator to a textual indicator, or allowing surgeons to turn it on and off.

The least appreciated elements of NeuroLens were the hologram personalization and the voice commands (51.5% and 48.5% positivity rates, correspondingly). We expect hologram personalization to be more important for other, more complex, AR-supported surgical settings: in our trials, the participants did not personalize holograms as the ventricular hologram provided sufficient information and none of the ventricular parts obstructed the surgical area. While we believe that voice commands will have an important role in AR-assisted surgery of the future, their usability in NeuroLens was limited by their lack of robustness: in our trials, the performance of the built-in voice recognition in HoloLens 2 was highly dependable on the noise

in the environment, which required many participants to repeat voice commands, often multiple times.

AR & surgical experience. The participants largely agreed that the provided visualizations did not obstruct their field of view (positivity rate: 87.9%), and that there was no noticeable lag in the system (positivity rate: 69.7%). A significant number of the participants did observe drifting or jumping of the rendered virtual contents (positivity rate: 45.5%). In the open-ended feedback, some participants additionally noted that they felt the catheter hologram “jumped” (P3, P14) and that it was hard to keep it steady (P1, P6). From our observations, instances of drifting or jumping were associated with specific scenarios, such as tracked objects coming in close proximity to one another or optical markers being blocked by the user; the prevalence of these scenarios was highly dependent on a specific participant’s approach to catheter placement. In future work, we will further investigate these scenarios, and will examine to what extent they can be addressed via technical solutions (e.g., further optimizing placement of the markers and the OptiTrack cameras) and via providing additional instructions to the users of our system (e.g., instructing the users to avoid obstructing the markers).

The participants agreed with the usefulness of NeuroLens in clinical settings (positivity rate: 90.0%) and the usefulness of phantom model for learning (positivity rate: 93.9%). However, only 69.7% of the participants agreed or strongly agreed that our phantom model was realistic; we are developing a more realistic model in our ongoing work. Additionally, 39.4% of the participants agreed or strongly agreed that the texture feedback provided in NeuroLens was realistic, with 47.1% being neutral; we believe this is due to the majority of participants having limited clinical experience that would allow them to assess the realism of this element of NeuroLens. In future work, we will recruit experienced neurosurgeons to provide a more comprehensive evaluation of NeuroLens as a learning tool.

Physical discomfort. By and large, the participants agreed or strongly agreed that the system was robust without discomfort (positivity rate: 93.9%), dizziness (positivity rate: 93.9%), and fatigue (positivity rate: 78.8%). The positivity rate for fatigue in NeuroLens was at a close level (75% - “visual fatigue”) to another reported AR-assisted EVD system [39]. In future work, we will examine which specific types of fatigue are experienced by the users of NeuroLens (e.g., it could be associated with eye discomfort, or with wearing an uncomfortably-fitting headset), and will develop approaches for addressing it. For example, we could provide users with instructions to rest, or reduce the amount of visual information presented to the users based on their level of fatigue.

Additional feedback. While participants’ accuracy was, on average, considerably improved when NeuroLens was used (see Fig. 6c),

Table 3: Comparison between groups that achieved different levels of accuracy on AR-assisted trials.

Criteria	Groups based on Performance		
	Best	Intermediate	Worst
Total number of participants	13	13	7
Number of year 1 students	7	7	5
Number of year 2–4 students	6	6	2
Average accuracy of AR-assisted EVD (mm)	3.89	11.5	21.3
Average completion time of AR-assisted EVD (s)	368.6	343.4	199.2
Average eye gaze focus on contextual guidance (%)	47.76	39.57	31.48
Positivity rate of survey responses on contextual guidance (%)	84.6	79.5	47.6
Positivity rate of survey responses on physical discomfort (%)	69.2	76.9	100

multiple participants have indicated that the core challenges of accurate EVD placement do not fundamentally change with the addition of AR guidance: specifically, the participants felt that finding the correct depth (P2, P19, P26), getting to the correct angle of insertion (P4, P5, P15, P20, P29), and estimating the target location (P12, P18) were still challenging. This is intuitive: while the contextual guidance NeuroLens provides can help guide the surgeons’ approach to the target and improve surgeons’ accuracy, the core task of hitting a small target, in an enclosed space, through a narrow opening, remains challenging regardless.

Overwhelmingly, the participants were positive about AR as a technology and its potential impact on neurosurgical applications. The participants thought the system was “a great, realistic tool for minimally invasive surgery” (P9), “great technology” (P15, P29), and “amazing tool for training, prep, and intraoperatively” (P17). One participant was “looking forward to seeing the technology progress” (P14). The participants also stated that “this was really cool” (P1, P5, P20, P27), “this was very useful” (P5, P22, P33), “great experiment” (P23), and “great learning experience” (P1). The enthusiasm of medical students further indicates NeuroLens’s potential as a tool that will aid and educate novice neurosurgeons.

5.5 Analysis based on Performance

We observed curious dissimilitude in the levels of accuracy achieved by different participants, and thus evaluated a range of metrics for the three distinct groups of participants. The *best-performing* group is made up of 13 participants whose accuracy on AR-assisted trials was under 7mm (average accuracy: 3.89mm). The *intermediate-performing* group is made up of 13 participants whose accuracy on AR-assisted trials was higher than 7mm, but performing better in AR-assisted than freehand EVD (average accuracy: 11.5mm). The *worst-performing* group is made up of 7 participants who performed worse on AR-assisted than freehand EVD (average accuracy: 21.3mm). These results are summarized in Table 3. We observed multiple notable differences between these groups. First, the groups that achieved better accuracy spent considerably more time on the task: to complete EVD catheter insertion, the best-performing group took 25 seconds more than the intermediate-performing group, and 169 seconds (*i.e.*, 85%) more than the worst-performing group. Second, eye gaze tracking indicates that the worst-performing group paid less attention to the provided contextual guidance than the other groups. *This may indicate that the average accuracy of AR-assisted surgery can be improved by instructing the participants to be slower and more deliberate in their actions, and to focus more on the provided contextual guidance.* However, we also saw a notable difference in the levels of self-reported physical discomfort in visual fatigue

among these groups: while 100% of the participants in the worst-performing group agreed or strongly agreed that they experienced no discomfort, that was the case for only 69.2% of the best-performing group. The observed link between performance and discomfort calls for further investigation of both qualitative and quantitative metrics of different types of discomfort (*e.g.*, physical, visual), in settings with longer and more complex neurosurgical procedures.

6 DISCUSSION AND FUTURE WORK

Currently, NeuroLens relies on optical marker-based tracking of the EVD catheter to integrate contextual guidance in visualizing the angle, distance to the target, and projection of catheter trajectory. Our current approach assumes that the inner stylet (which surgeons insert inside the catheter) does not bend; when it does, our system provides incorrect guidance to the surgeons. To address this, we plan to embed sensors such as strain gauges [20] or use a computer vision algorithm [37] to accurately capture the shape of the inner stylet to further improve the accuracy of our AR-based guidance.

So far, we have designed NeuroLens to provide contextual guidance only in catheter placement; however, EVD entails the whole process of identifying external landmarks, drilling Kocher’s points (*i.e.*, *craniotomy*), and determining the catheter trajectory. We will expand our contextual guidance by identifying external landmarks such as medial canthus and tragus [13, 18] in real-time using AR by integrating OpenCV with HoloLens 2 to guide surgeons in planning of drilling Kocher’s points at optimal locations [3]. Additionally, to evaluate this, we will develop a more realistic patient-specific phantom model and enhance the emulation of the brain texture [21].

We have evaluated NeuroLens for training medical students to improve catheter placement accuracy with a future goal of clinical implementation; however, the current NeuroLens setup in a clinical setting has limitations in 1) space constraints due to the external camera setup taking too much space, 2) time constraints due to manual image segmentation [28, 42], and 3) robustness of real-time registration due to occlusion or loss of markers [6, 42]. To address the space constraint, we plan to mount the OptiTrack cameras on the ceiling to declutter the surgical area [10, 16]. To reduce the preparation time, we will develop an automatic image segmentation of the brain ventricles from the CT scans. Lastly, we will use OptiTrack’s Motion Capture suit [24] for developing a more robust marker model that can tolerate the occlusion of markers in specific scenarios.

7 CONCLUSIONS

This paper presents NeuroLens, the first AR-based contextual guidance system that guides neurosurgeons in the catheter placement of the EVD procedure. NeuroLens provides both the anatomical visualization of the patient’s ventricular hologram and the guidance on catheter placement, enabled by tracking the catheter. Our evaluations of NeuroLens with 33 medical students, who used NeuroLens to insert an EVD catheter used in clinical settings into a realistic phantom model of a human head, demonstrated that NeuroLens helped students place the catheter closer to its target. Furthermore, our study demonstrated that participants who focused more on the provided guidance achieved higher accuracy. In future work, we will develop approaches to EVD catheter tracking that take the catheter’s non-rigidity into account, and will design, develop, and evaluate a wide range of additional contextual guidance for the surgeons.

ACKNOWLEDGMENTS

We thank Seijung Kim and Ritvik Janamsetty for their work on this project. We also thank all participants in our user study. This work was supported in part by NSF grants CNS-2112562 and CNS-1908051, NSF CAREER Award IIS-2046072, by a Thomas Lord Educational Innovation Grant, and by an AANS Neurosurgery Technology Development Grant.

REFERENCES

- [1] Y. Adagolodjo, N. Golse, E. Vibert, M. De Mathelin, S. Cotin, and H. Courtecuisse. Marker-based registration for large deformations-application to open liver surgery. In *Proc. IEEE ICRA*, 2018.
- [2] A. AlAzri, K. Mok, J. Chankowsky, M. Mullah, and J. Marcoux. Placement accuracy of external ventricular drain when comparing freehand insertion to neuronavigation guidance in severe traumatic brain injury. *Acta Neurochirurgica*, 159(8):1399–1411, 2017.
- [3] M. O. Alves and D. O. Dantas. Mobile augmented reality for craniotomy planning. In *Proc. IEEE ISCC*, 2021.
- [4] C. M. Andrews, A. B. Henry, I. M. Soriano, M. K. Southworth, and J. R. Silva. Registration techniques for clinical applications of three-dimensional augmented reality devices. *IEEE Journal of Translational Engineering in Health and Medicine*, 9:1–14, 2020.
- [5] L. Chen, T. W. Day, W. Tang, and N. W. John. Recent developments and future challenges in medical mixed reality. In *Proc. IEEE ISMAR*, 2017.
- [6] S. Chidambaram, V. Stifano, M. Demetres, M. Teyssandier, M. C. Palumbo, A. Redaelli, A. Olivi, M. L. Apuzzo, and S. C. Pannullo. Applications of augmented reality in the neurosurgical operating room: a systematic review of the literature. *Journal of Clinical Neuroscience*, 91:43–61, 2021.
- [7] S. Eom, S. Kim, S. Rahimpour, and M. Gorlatova. AR-assisted surgical guidance system for ventriculostomy. In *Proc. IEEE VR Workshops*, 2022.
- [8] T. Fick, J. van Doormaal, E. Hoving, L. Regli, and T. van Doormaal. Holographic patient tracking after bed movement for augmented reality neuronavigation using a head-mounted display. *Acta Neurochirurgica*, 163(4):879–884, 2021.
- [9] T. Frantz, B. Jansen, J. Duerinck, and J. Vandemeulebroucke. Augmenting Microsoft’s HoloLens with Vuforia tracking for neuronavigation. *Healthcare Technology Letters*, 5(5):221–225, 2018.
- [10] D. Gasques, J. G. Johnson, T. Sharkey, Y. Feng, R. Wang, Z. R. Xu, E. Zavala, Y. Zhang, W. Xie, X. Zhang, et al. ARTEMIS: A collaborative mixed-reality system for immersive surgical telementoring. In *Proc. ACM CHI*, 2021.
- [11] M. S. Greenberg and N. Arredondo. *Handbook of Neurosurgery*, vol. 87. Thieme New York, 2001.
- [12] C. Gsaxner, J. Li, A. Pepe, D. Schmalstieg, and J. Egger. Inside-out instrument tracking for surgical navigation in augmented reality. In *Proc. ACM VRST*, 2021.
- [13] C. Gsaxner, A. Pepe, J. Wallner, D. Schmalstieg, and J. Egger. Markerless image-to-face registration for untethered augmented reality in head and neck surgery. In *International Conference on Medical Image Computing and Computer-Assisted Intervention*. Springer, 2019.
- [14] D. Guha, N. M. Alotaibi, N. Nguyen, S. Gupta, C. McFaul, and V. X. Yang. Augmented reality in neurosurgery: a review of current concepts and emerging applications. *Canadian Journal of Neurological Sciences*, 44(3):235–245, 2017.
- [15] J. Haemmerli, A. Davidovic, T. R. Meling, L. Chavaz, K. Schaller, and P. Bijlenga. Evaluation of the precision of operative augmented reality compared to standard neuronavigation using a 3D-printed skull. *Neurosurgical Focus*, 50(1):E17, 2021.
- [16] M. Kanegae, J. Morita, S. Shimamura, Y. Uema, M. Takahashi, M. Inami, T. Hayashida, and M. Sugimoto. Registration and projection method of tumor region projection for breast cancer surgery. In *Proc. IEEE VR*, 2015.
- [17] D. Katić, P. Spengler, S. Bodenstedt, G. Castrillon-Oberndorfer, R. Seeburger, J. Hoffmann, R. Dillmann, and S. Speidel. A system for context-aware intraoperative augmented reality in dental implant surgery. *International Journal of Computer Assisted Radiology and Surgery*, 10(1):101–108, 2015.
- [18] C. Leuze, S. Sathyanarayana, B. L. Daniel, and J. A. McNab. Landmark-based mixed-reality perceptual alignment of medical imaging data and accuracy validation in living subjects. In *Proc. IEEE ISMAR*, 2020.
- [19] Y. Li, X. Chen, N. Wang, W. Zhang, D. Li, L. Zhang, X. Qu, W. Cheng, Y. Xu, W. Chen, et al. A wearable mixed-reality holographic computer for guiding external ventricular drain insertion at the bedside. *Journal of Neurosurgery*, 131(5):1599–1606, 2018.
- [20] M. A. Lin, A. F. Siu, J. H. Bae, M. R. Cutkosky, and B. L. Daniel. HoloNeedle: augmented reality guidance system for needle placement investigating the advantages of three-dimensional needle shape reconstruction. *IEEE Robotics and Automation Letters*, 3(4):4156–4162, 2018.
- [21] E. C. Mackle, J. Shapey, E. Maneas, S. R. Saeed, R. Bradford, S. Ourselin, T. Vercauteren, and A. E. Desjardins. Patient-specific polyvinyl alcohol phantom fabrication with ultrasound and X-ray contrast for brain tumor surgery planning. *Journal of Visualized Experiments*, (161):e61344, 2020.
- [22] A. Meola, F. Cutolo, M. Carbone, F. Cagnazzo, M. Ferrari, and V. Ferrari. Augmented reality in neurosurgery: a systematic review. *Neurosurgical Review*, 40(4):537–548, 2017.
- [23] R. Muralidharan. External ventricular drains: Management and complications. *Surgical Neurology International*, 6(Suppl 6):S271, 2015.
- [24] NaturalPoint. OptiTrack – motion capture suits. <https://optitrack.com/accessories/wear/>, 2022.
- [25] H. Ofoma, B. Cheaney II, N. J. Brown, B. V. Lien, A. S. Himstead, E. H. Choi, S. Cohn, J. K. Campos, and M. Y. Oh. Updates on techniques and technology to optimize external ventricular drain placement: A review of the literature. *Clinical Neurology and Neurosurgery*, 213:107126, 2022.
- [26] B. R. O’Neill, D. A. Velez, E. E. Braxton, D. Whiting, and M. Y. Oh. A survey of ventriculostomy and intracranial pressure monitor placement practices. *Surgical Neurology*, 70(3):268–273, 2008.
- [27] M. Pishjoo, K. Khatibi, H. Etemadzezaie, S. Zabihiyan, B. Ganjeifar, M. Safdari, and H. Baharvahdat. Determinants of accuracy of freehand external ventricular drain placement by neurosurgical trainees. *Acta Neurochirurgica*, 163(4):1113–1119, 2021.
- [28] Z. Qi, Y. Li, X. Xu, J. Zhang, F. Li, Z. Gan, R. Xiong, Q. Wang, S. Zhang, and X. Chen. Holographic mixed-reality neuronavigation with a head-mounted device: technical feasibility and clinical application. *Neurosurgical Focus*, 51(2):E22, 2021.
- [29] L. Qian, A. Deguet, Z. Wang, Y.-H. Liu, and P. Kazanzides. Augmented reality assisted instrument insertion and tool manipulation for the first assistant in robotic surgery. In *Proc. IEEE ICRA*, 2019.
- [30] N. Rewkowski, A. State, and H. Fuchs. Small marker tracking with low-cost, unsynchronized, movable consumer cameras for augmented reality surgical training. In *Proc. IEEE ISMAR-Adjunct*, 2020.
- [31] M. Schneider, C. Kunz, A. Pal’ a, C. R. Wirtz, F. Mathis-Ullrich, and M. Hlaváč. Augmented reality–assisted ventriculostomy. *Neurosurgical Focus*, 50(1):E16, 2021.
- [32] W. Si, X. Liao, Q. Wang, and P.-A. Heng. Augmented reality-based personalized virtual operative anatomy for neurosurgical guidance and training. In *Proc. IEEE VR*, 2018.
- [33] S. Skyрман, M. Lai, E. Edström, G. Burström, P. Förander, R. Homan, F. Kor, R. Holthuisen, B. H. Hendriks, O. Persson, et al. Augmented reality navigation for cranial biopsy and external ventricular drain insertion. *Neurosurgical Focus*, 51(2):E7, 2021.
- [34] SMiF. High resolution X-ray computed tomography scanner. <https://smif.pratt.duke.edu/node/153>, 2022.
- [35] T. Song, C. Yang, O. Dianat, and E. Azimi. Endodontic guided treatment using augmented reality on a head-mounted display system. *Healthcare Technology Letters*, 5(5):201–207, 2018.
- [36] M. Stuart, J. Antony, T. Withers, and W. Ng. Systematic review and meta-analysis of external ventricular drain placement accuracy and narrative review of guidance devices. *Journal of Clinical Neuroscience*, 94:140–151, 2021.
- [37] X. Sun, S. B. Murthi, G. Schwartzbauer, and A. Varshney. High-precision 5DoF tracking and visualization of catheter placement in EVD of the brain using AR. *ACM Transactions on Computing for Healthcare*, 1(2):1–18, 2020.
- [38] P. Tu, Y. Gao, A. J. Lungu, D. Li, H. Wang, and X. Chen. Augmented reality based navigation for distal interlocking of intramedullary nails utilizing Microsoft HoloLens 2. *Computers in Biology and Medicine*, 133:104402, 2021.
- [39] F. Van Gestel, T. Frantz, C. Vannerom, A. Verhellen, A. G. Gallagher, S. A. Elprama, A. Jacobs, R. Buyil, M. Bruneau, B. Jansen, et al. The effect of augmented reality on the accuracy and learning curve of

external ventricular drain placement. *Neurosurgical Focus*, 51(2):E8, 2021.

- [40] N. Weibel, D. Gasques, J. Johnson, T. Sharkey, Z. R. Xu, X. Zhang, E. Zavala, M. Yip, and K. Davis. ARTEMIS: mixed-reality environment for immersive surgical telementoring. In *Proc. ACM CHI Extended Abstracts*, 2020.
- [41] J. Woodward and J. Ruiz. Analytic review of using augmented reality for situational awareness. *IEEE Transactions on Visualization and Computer Graphics*, 2022.
- [42] G. Yavas, K. E. Caliskan, and M. S. Cagli. Three-dimensional-printed marker-based augmented reality neuronavigation: a new neuronavigation technique. *Neurosurgical Focus*, 51(2):E20, 2021.